ISSN 1063-7826, Semiconductors, 2013, Vol. 47, No. 12, pp. 1598–1603. © Pleiades Publishing, Ltd., 2013.
Original Russian Text © A.V. Larionov, A.I. Il'in, 2013, published in Fizika i Tekhnika Poluprovodnikov, 2013, Vol. 47, No. 12, pp. 1624–1629.

SYMPOSIUM
"NANOPHYSICS AND NANOELECTRONICS",
NIZHNI NOVGOROD, MARCH, 2013 (CONTINUATION)

Laterally Localizing Potential as a Tool for Controlling the Electron Spin Relaxation Time in GaAs Quantum Wells

A. V. Larionov[a]^ and A. I. Il'in[b]

[a] *Institute of Solid State Physics, Russian Academy of Sciences, Chernogolovka, Moscow oblast, 142432 Russia*
^e-mail: larionov@issp.ac.ru
[b] *Institute of Microelectronics Technology and High-Purity Materials, Russian Academy of Sciences, Chernogolovka, Moscow oblast, 142432 Russia*

Submitted April 22, 2013; accepted for publication April 30, 2013

Abstract—The coherent spin dynamics of electrons localized in a plane of GaAs quantum wells is studied experimentally by the application of an electrically controlled potential. The localizing potential is produced with the use of a metal gate with submicrometer windows deposited onto the sample surface. The photoinduced spin Kerr effect is used to study the electron spin lifetime as a function of the temperature, applied bias, and magnetic field for gates with different sets of windows. It is shown that, with an electrically controlled laterally localizing potential, it is possible to gradually change the electron spin lifetime from several hundreds of picoseconds to several tens of nanoseconds. The dependence of the electron spin relaxation time on the sizes of the lateral localization region is in good qualitative agreement with theoretical prediction.

DOI: 10.1134/S1063782613120142

1. INTRODUCTION

Monitoring and controlling the charge-carrier spin degrees of freedom are one of the main fields and problems of studies in spintronics (see, e.g., [1–3]). In the case of nonmagnetic semiconductor structures, influence on the charge-carrier spin is possible due to the spin–orbit interaction. In semiconductor crystals without a symmetry center (III–V, II–VI semiconductors), the spin–orbit interaction induces an energy gap [4] in the spectrum of charge carriers, and this gap can be considered as an effective magnetic field. As a consequence, a new mechanism of spin relaxation (Dyakonov–Perel's mechanism) appears due to electron (or hole) precession in this effective magnetic field. In two-dimensional semiconductor structures, i.e., quantum wells (QWs), additional spin–orbit splitting emerges due to Rashba's effect associated with the asymmetry of the semiconductor structure along the growth axis (structural inversion asymmetry). The spin–orbit splitting induced by the structural inversion asymmetry (Rashba's Hamiltonian) and the splitting that emerges due to the bulk structural asymmetry (Dresselhaus's Hamiltonian) can interfere in the direction of certain crystallographic axes orthogonal to the growth axis of the heterostructure [5]. This interference and, hence, spin–orbit splitting can be controlled with an applied external bias [6]; in this manner, one can influence the mechanism of spin relaxation and, thus, change the spin lifetime. Such influence on spin–orbit splitting is rather limited in strength and the electron spin lifetime can be changed in the range from several hundreds of picoseconds to few nanoseconds. Several years ago, another method making it possible to efficiently control the spin–orbit interaction was proposed. The basic idea of this method is to provide the artificial confinement of electron motion in the QW plane; as a result, the effect of the effective magnetic field dependent on the electron momentum on the electrons is dramatically reduced even at a length scale of ~1 μm. Specifically, Kiselev and Kim [7] theoretically predicted that, by changing the width of the two-dimensional channel or by confining charge-carrier motion along one direction in the lateral plane, for example, by means of etching micrometer-wide strips in the two-dimensional channel, it is possible to change the electron spin lifetime by several orders of magnitude. Qualitatively, this prediction was supported experimentally by Holleitner et al. [8], who studied the electron spin dynamics in GaAs QWs with different two-dimensional channel widths.

In our view, a more promising method is to the use of the three-dimensional confinement of electron motion by producing electrically controlled lateral potential wells, as proposed by Nikolyuk and Ignatiev [9]. To control the orbital electron motion in the QW plane, it was suggested [9] that quantum-confined lateral potential traps for electrons be formed by applying an electrical bias to a specially shaped electrode, specifically, a mosaic electrode produced on the nanostructure surface. In essence, such traps are electri-

cally induced quantum dots, in which the electron spin lifetime can reach several hundreds of nanoseconds, as estimated in [9]. However, as predicted theoretically in [10], the length scale of lateral electron localization needed for efficient suppression of Dyakonov–Perel's mechanism can exceed the length scale of quantum confinement by an order of magnitude and correspond to several hundreds of nanometers. Previously, we have shown (see [11–13]) that the use of electrically controlled lateral potential traps yields a substantial increase in the electron spin relaxation time. An ensemble of such potential nanotraps may be a new class of induced quantum dots (IQDs). In combination with high-quality GaAs QWs, IQDs can offer considerable promise for practical use as the basic element of spin memory cells. This study presents an experimental investigation of the electron spin lifetime in relation to lateral potential trap sizes, applied electrical bias, magnetic field, and temperature.

2. EXPERIMENTAL

The experiments were conducted for GaAs nanostructures formed as Schottky photodiodes, in which the role of the internal electrode was played by a 30-nm-wide Si-doped GaAs QW and the external Schottky gate was a special electrode with a regular ensemble of submicrometer windows (the mosaic gate). An electrical bias was created between the internal electrode and the external Schottky gate at the surface of the GaAs nanostructure. Between the two gates, symmetrically with respect to them, a single 25- or 40-nm-wide GaAs QW separated from the gates by a ~200-nm-thick insulator AlGaAs layer was arranged. The mosaic gate was made of a 80-nm-thick gold film 100×100 μm in size, with a regular array of windows 1.7, 1.2, 0.8, 0.6, and 0.4 μm in diameter; the windows were arranged as a close-packed triangular lattice, in which the spacing between the window centers was, correspondingly, 2.2, 1.6, 1.2, 0.9, and 0.6 μm (see Fig. 1). To form the mosaic electrode from the gold film on the GaAs substrate, we used an original procedure that involved both electronic lithography and lift-off lithography. Electron lithography was implemented with an EVO-50 scanning electron microscope equipped with a NanoMaker software/hardware system. For comparative measurements, a ~20-nm-thick semitransparent gold electrode was attached to the agregate structure.

The sample to be studied was placed into an optical cryostat with a solenoid that allowed us to apply magnetic fields of up to $B = 6$ T and to use the transverse geometrical layout of the magnetic field (Voigt layout) at 2 K. The electron spin dynamics was studied by the method of the photoinduced magnetooptic Kerr rotation effect. For the photoexcitation source, we used a femtosecond pulsed titanium–sapphire laser (operating at a pulse frequency of 82 MHz). To obtain a spectrally narrow pulse (with a spectral width of ~0.5 meV),

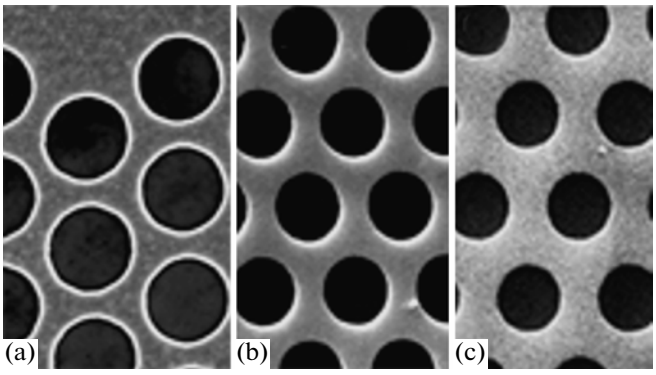

Fig. 1. Fragments of images of the mosaic gates with the window sizes (a) 1.7, (b) 1.2, and (c) 0.8 μm. The images are recorded with an EVO-50 scanning electron microscope.

we used a special tunable electrooptic filter that selected the required spectral region in the wide femtosecond-pulse spectrum. Then the laser pulse was split into two parts, the pump pulse and the probe pulse. The average powers of the pump and probe pulses were, correspondingly, ~1 and ~0.5 mW at the laser spot on the sample surface 100 μm in size. The circularly polarized pump pulse induced spin orientation in the sample. The orientation was detected from the rotation angle of the polarization plane of the linearly polarized probe beam reflected from the sample; this was done with a special balanced photodetector. The measurements were conducted in the spectrally degenerate mode of operation, in which the wavelengths of the pump and probe laser beams were equal. The signal was detected by doubled locked-in detection that makes possible efficient suppression of the spurious signal produced by pumping light scattered from the mosaic electrode. To do this, we implemented additional (amplitude) modulation of the probe beam and detected the Kerr rotation signal at the corresponding modulation frequency. The mechanical delay line used in the experiments allowed us to conduct the measurements in the time interval between the pump and probe beams shorter than 6.7 ns.

3. RESULTS

Figure 2 shows the photoluminescence (PL) spectra integrated over time for the samples with the mosaic (Fig. 2a) and semitransparent (Fig. 2b) electrodes. The spectra were recorded upon quasi-resonance photoexcitation with a laser-radiation photon energy of ~10 meV higher than the energy of the 1sLH exciton state for the GaAs QW (25 nm). The PL spectra were recorded at different applied electrical bias varied in the range from 0 to 1.8 V with a step of 0.1 V. The bias polarity was positive; in this case, the applied electrical bias compensates the built-in electric field produced in structures involving Schottky diodes (the

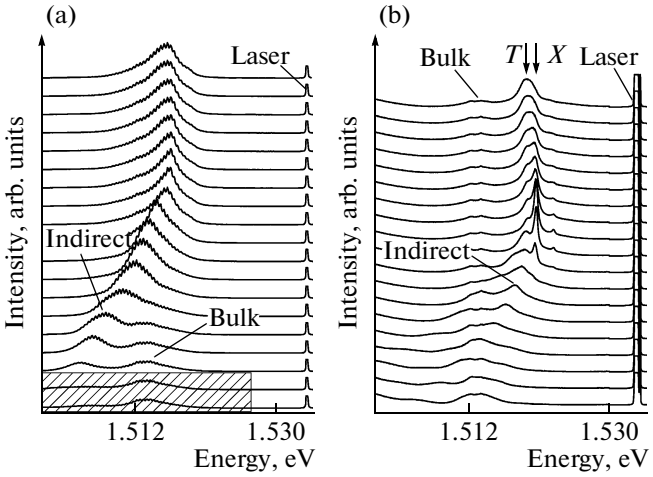

Fig. 2. PL spectra of the samples with (a) mosaic and (b) semitransparent electrodes at applied electrical biases varied (from bottom to top) in the range from 0 to 1.8 V with a step of 0.1 V. (a) shaded rectangle shows the transparency spectral region of the interference filter used to record the PL spectra emitted from the surface with the mosaic electrode. The windows in the mosaic electrode were 1.7 μm in size.

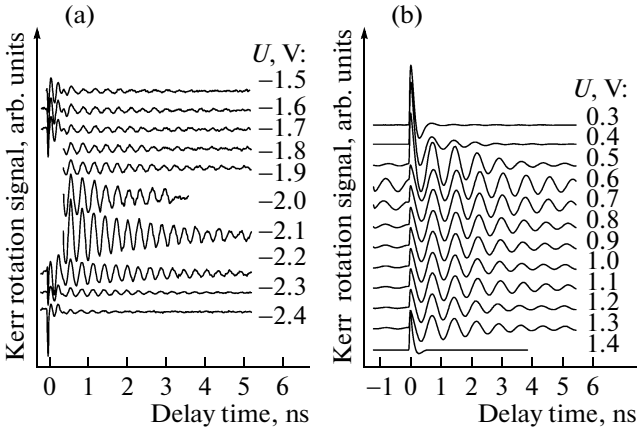

Fig. 3. The amplitude of the Kerr rotation signal versus the delay time of the probe pulse with respect to the pump pulse, as recorded at different applied biases U for GaAs QW nanostructures (25 nm) with surface mosaic electrodes with the window sizes (a) 1.7 and (b) 0.6 μm. The magnetic induction is B = (a) 0.75 and (b) 0.25 T. The applied biases U with the corresponding polarity are indicated.

blocking bias). It can be seen that, in the case of the mosaic electrode, the PL spectra exhibit only one feature that is associated with the GaAs QW (25 nm) and corresponds to the recombination of spatially separated electrons and holes (indirect recombination). Previously [14], it was shown that the external electrical bias created a potential well along the window perimeter, whereas the potential at the window center was much lower, though nonzero. In contrast to the results of [14], in the PL spectra shown in Fig. 2a, there is no line corresponding to the radiative recombination of the 1*sHH* exciton (line *X*) and there is no line corresponding to the radiative recombination of the exciton bound to a localized charge carrier (trion line *T*). These features are observed only in the PL spectra of the sample with the semitransparent electrode (Fig. 2b). This means that the electrical bias applied to the mosaic electrode apparently creates a potential well at the window center. This difference between the results obtained here and in [14] can be due only to the difference between the window sizes which are 1.7 μm here and 5 μm in [14]. The behavior of the PL spectra illustrated in Fig. 2 is characteristic of all of the GaAs QW (25 nm) nanostructures under study, irrespective of the size of the windows in the mosaic electrode. The distinct inhomogeneous broadening of the PL line is due to the nonunifirmity of the electric field inside the window in the mosaic electrode. From analysis of the PL excitation spectra, it is established that the above-discussed feature always emerges upon resonance excitation of the 1*sHH* exciton independently of the applied external bias.

Figure 3 shows the dynamics of electron spin polarization for different electrical biases applied to the mosaic electrode with window sizes of 1.7 (25 nm QW, Fig. 3a) and 0.6 μm (25 nm QW, Fig. 3b). The measurements were conducted at a constant laser-radiation photon energy that coincided with the spectral position of the 1*sHH* exciton. We studied the dependence of the amplitude of the Kerr rotation signal on the delay time of the probe pulse with respect to the pump pulse. It is found that there exist two different modes of electron spin dynamics depending on the size of the windows in the mosaic electrode. For the GaAs nanostructures with window sizes of 0.8–1.7 μm in the mosaic gate, the electron spin relaxation time is maximal at reverse bias (negative polarity, Fig. 3a). For the GaAs nanostructures with window sizes of 0.4–0.8 μm in the mosaic gate, the electron spin relaxation time is maximal at forward bias (positive, blocking polarity, Fig. 3b).

The periodic oscillations observed in the Kerr signal arise from the precession of coherently aligned electron spins about the external magnetic field. The precession frequency (Larmor frequency) Ω_L is determined as $\hbar\Omega_L = \Delta E = \mu_B g_e^{xy} B$. Here, ΔE is the electron spin splitting in the conduction band and g_e^{xy} is the electron g factor in the QW plane. From the data reported in publications, it is well known that, in such structures, the g factor g_e^{xy} is almost an order of magnitude larger than the corresponding quantity for holes g_h^{xy} and the spin relaxation time for holes is much shorter than that for electrons. Therefore, as in [6], we assume that the experimentally observed quantum beats occur between the electron spin states. The

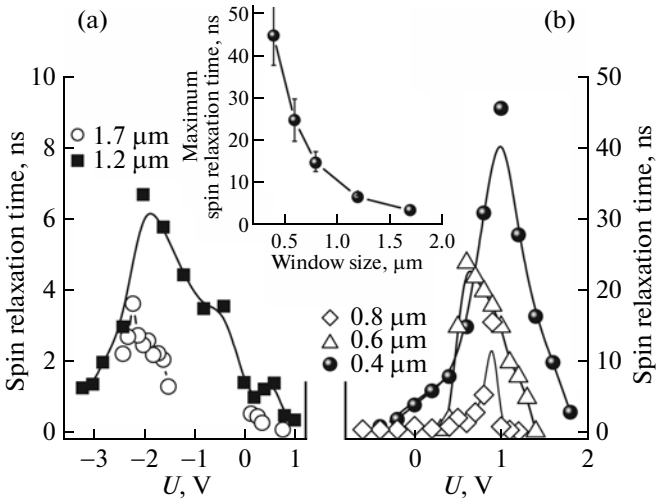

Fig. 4. Summary data on the dependence of the electron spin relaxation time upon the applied electrical bias U in GaAs QW nanostructures with mosaic electrodes with the window sizes (a) 1.7 and 1.2 μm and (b) 0.8, 0.6, and 0.4 μm. Inset: the dependence of the maximum electron spin relaxation time on the window size in the mosaic electrode.

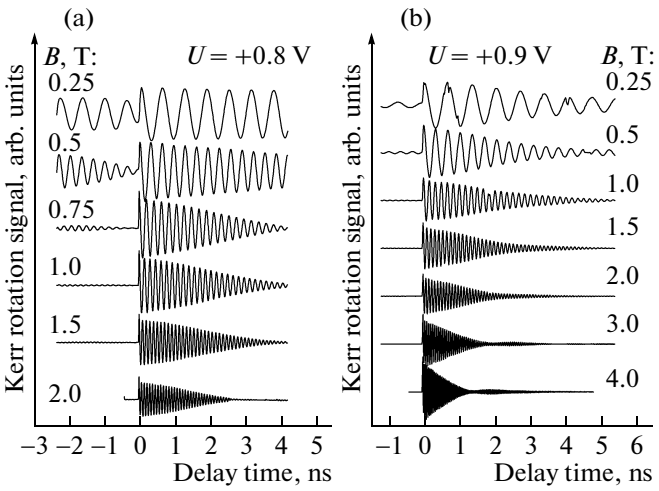

Fig. 5. The amplitude of the Kerr rotation signal versus the delay time of the probe pulse with respect to the pump pulse, as recorded at constant electrical biases U and different external magnetic fields B for GaAs QW nanostructures with mosaic electrodes with window sizes of (a) 0.4 (40 nm QW) and (b) 0.6 μm (0.25 nm QW).

experimental results shown in Fig. 3a were approximated by an oscillating dependence damped with time t in accordance with a single exponent, with the oscillation frequency Ω_L and the decay time T_S^e:

$$I = I_0 \exp(-t/T_S^e)\cos(\Omega_L t). \quad (1)$$

In the case of the GaAs nanostructures with 0.4–0.8 μm windows in the mosaic electrode, the electron spin dynamics are more complex and can be described by exponential decay with two different time constants, T_{S1}^e and T_{S2}^e:

$$I = I_{01}\exp(-t/T_{S1}^e)\cos(\Omega_L t)/[1 - \exp(-12.2/T_{S1}^e)] + I_{02}\exp(-t/T_{S2}^e)\cos(\Omega_L t)/[1 - \exp(-12.2/T_{S2}^e)]. \quad (2)$$

Here, the denominator is the sum of an infinite geometrical progression and the summation is carried out over all laser pulses emitted with the pulse period 12.2 ns. From the total set of experimental data, it is established that the time constant T_{S2}^e is most sensitive to the electrical bias.

Figure 4a shows summary data on the dependence of the spin relaxation time on the applied bias for the GaAs nanostructures with different arrays of windows in the mosaic electrode, as obtained in accordance with expressions (1) and (2). It can be seen that, as the window size is reduced, the spin relaxation time becomes substantially (several times) longer. Figure 4b shows the maximum spin relaxation time as a function of the window size in the mosaic electrode.

Figure 5 shows the Kerr curves obtained for the GaAs nanostructures with different arrays of windows in the mosaic electrode at certain applied biases and different external magnetic fields. An increase in the magnetic field yields a sharp decrease in the spin relaxation time, which is attributed to the large dispersion of the electron g factor. The experimentally observed magnetic-field dependence is rather typical of self-assembled quantum dots (QDs) (see, e.g., [15]) and of QWs with high amplitudes of the random potential laterally localizing electrons (see [16]).

In addition, we here studied the anisotropy of the electron spin relaxation in the case of a mosaic electrode (Fig. 6). The measurements were conducted at a constant external electrical bias and at a constant magnetic field. We gradually varied the angle between the direction of the magnetic field and the [110] crystallographic direction. From Fig. 6b, it can be seen that the spin relaxation time is highly anisotropic. The character of the anisotropy differs dramatically from that observed previously for a GaAs QW (25 nm) nanostructure with 1.7 μm windows in the mosaic electrode [12]. The angular dependence obtained here is no longer described by the equation for anisotropic spin dynamics in QWs (see [6]) and is characteristic of QDs (see, e.g., [17]).

In order to estimate the localizing potential, we conducted temperature measurements of the spin relaxation time (see Fig. 7). From the activation dependence of the amplitude of the Kerr signal on the inverse temperature, we can estimate the activation energy at 2 meV (see [18] for a similar estimate). We suppose that this value gives an estimate for the average depth of lateral potential wells, since the binding energy of localized electrons in the structures under consideration is <1 eV. Dependences similar to those

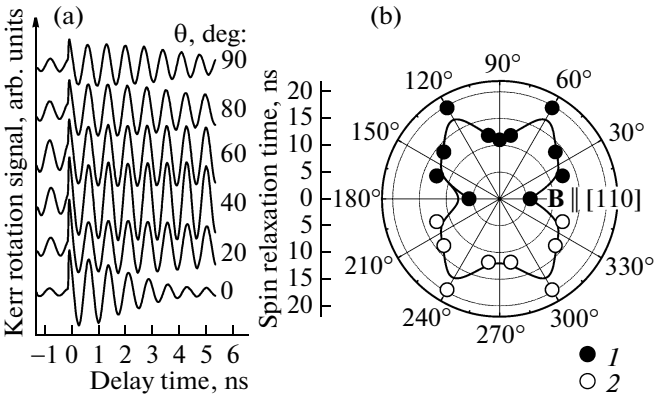

Fig. 6. (a) Amplitude of the Kerr signal recorded for the GaAs QW (25 nm) nanostructure at different angles θ between the direction of the magnetic field and the [110] crystallographic direction. The magnetic field is B = 0.25 T and the electrical bias is U = +0.6 V. The window size in the mosaic electrode is 0.6 μm. (b) The electron spin relaxation time (*1*) as a function of the angle φ and (*2*) as a function of φ extrapolated from symmetry considerations. The solid curve serves as a guide for the eye.

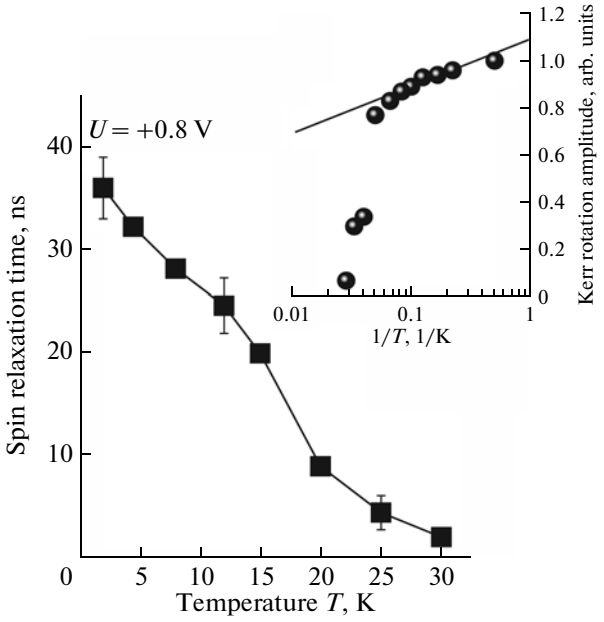

Fig. 7. Dependence of the electron spin relaxation time on temperature T for the GaAs QW nanostructure with the mosaic electrode with a window size of 0.4 μm (40 nm QW) at a constant electrical bias U. The inset shows the amplitude of the Kerr rotation signal versus the inverse temperature T^{-1}; the straight line corresponds to the activation energy ~2 meV.

shown in Fig. 7 were obtained for this nanostructure also at other applied biases, and qualitatively, these dependences behave similarly.

4. DISCUSSION

From analysis of the set of experimental data obtained in the study, we can conclude that the electrical bias applied to the GaAs nanostructure with a mosaic metal electrode on the surface creates a single potential well at the center of the window of the mosaic electrode and this well captures electrons. The depth of such a lateral potential trap is defined by the magnitude of the applied reverse or forward bias, and the lateral size depends on the window diameter. As the potential trap size is reduced, the spin relaxation time sharply increases following a superlinear dependence, which is due to suppression of Dyakonov–Perel's mechanism of spin relaxation, as predicted theoretically in [10]. For this effect to occur, no quantum-confinement length scale of the lateral trap is needed: the spin relaxation is efficiently suppressed even in the case of submicrometer trap sizes. The experimental dependence of the spin relaxation time on the size of the lateral electron localization region (see inset in Fig. 4) is in good agreement with the theoretically derived quadratic dependence (formula (19) in [10]).

In addition, from the experimental data obtained here, it follows that, depending on the lateral trap size, long-term spin memory can be inherent in both photoexcited electrons (at window sizes of >1 μm in the mosaic electrode, as evident from Fig. 4a) and resident electrons (at the window sizes <1 μm, as evident from Fig. 4b). At low temperatures, resident electrons are apparently localized at D^0X complexes.

From the temperature dependences of the Kerr signal amplitude and spin relaxation time, we can estimate the potential trap depth at 2 meV. At the same time, as follows from the PL spectra, the binding energy of electrons at D^0X complexes does not exceed 1 meV for the QWs under study. The potential-trap depth is defined by the architecture of the nanostructure and can vary in accordance with the GaAs QW depth with respect to the surface.

The decrease in the spin relaxation time with increasing magnetic field is due to the dispersion of the electron g factor; the spread is larger for smaller window sizes in the mosaic electrode. This effect arises from an increase in the degree of nonuniformity of the electric field inside the window, resulting in a larger dispersion of the potential-well depth, in which electrons are localized. The high anisotropy of spin relaxation and its symmetry are indicative of the important role of the shape of the lateral trap, in which electrons are localized.

The above-proposed method of the electrically controlled localization of electrons can serve as a new efficient tool for controlling spin–orbit interaction in GaAs QW nanostructures.

5. CONCLUSIONS

Thus, in this study, the coherent spin dynamics of electrons localized in the plane of GaAs QWs, in artificially produced and electrically controlled lateral traps is explored. It is shown that, with a mosaic gate at the surface of the GaAs nanostructures, it is possible to vary the electron spin relaxation time by two orders of magnitude (from ~500 ps to ~50 ns). This result is one of the records at present. The experimentally obtained dependence of the spin relaxation time on the sizes of the lateral localization region is in good qualitative agreement with the theoretically predicted dependence.

ACKNOWLEDGMENTS

We thank M.M. Glazov for useful discussion and remarks. We also thank V. Murav'ev for his help in fabricating electrical contacts to the samples.

The study was supported by the Russian Foundation for Basic Research, project no. 11-02-12289.

REFERENCES

1. G. Lommer, F. Malcher, and U. Roessler, Phys. Rev. Lett. **60**, 728 (1988).
2. S. Datta and B. Das, Appl. Phys. Lett. **56**, 665 (1990).
3. Y. Kato, R. C. Myers, A. C. Gossard, and D. D. Awschalom, Nature **42**, 50 (2004).
4. G. Dresselhaus, Phys. Rev. **100**, 580 (1955).
5. N. S. Averkiev, L. E. Golub, A. S. Gurevich, V. P. Evtikhiev, V. P. Kochereshko, A. V. Platonov, A. S. Shkolnik, and Yu. P. Efimov, Phys. Rev. B **74**, 033305 (2006).
6. A. V. Larionov and L. E. Golub, Phys. Rev. B **78**, 033302 (2008).
7. A. Kiselev and K. W. Kim, Phys. Rev. B **61**, 13115 (2000).
8. A. W. Holleitner, V. Sih, R. C. Myers, A. C. Gossard, and D. D. Awschalom, New J. Phys. **9**, 342 (2007).
9. V. A. Nikolyuk and I. V. Ignatiev, Semiconductors **41**, 1422 (2007).
10. I. S. Lyubinskii, JETP Lett. **83**, 336 (2006).
11. R. V. Cherbunin, M. S. Kuznetsova, I. Ya. Gerlovin, I. V. Ignat'ev, Yu. K. Dolgikh, Yu. P. Efimov, S. A. Eliseev, V. V. Petrov, S. V. Poltavtsev, A. V. Larionov, and A. I. Il'in, Phys. Solid State **51**, 837 (2009).
12. A. V. Larionov, A. V. Sekretenko, and A. I. Il'in, JETP Lett. **93**, 269 (2011).
13. A. V. Larionov, A. V. Sekretenko, and A. I. Il'in, Solid State Commun. **152**, 1893 (2012).
14. A. V. Gorbunov and V. B. Timofeev, JETP Lett. **84**, 329 (2006).
15. I. A. Yugova, A. Greilich, D. R. Yakovlev, A. A. Kiselev, M. Bayer, V. V. Petrov, Yu. K. Dolgikh, D. Reuter, and A. D. Wieck, Phys. Rev. B **75**, 245302 (2007).
16. A. V. Larionov and A. V. Sekretenko, JETP Lett. **94**, 853 (2011).
17. A. Schwan, A. Greilich, D. R. Yakovlev, M. Bayer, A. D. B. Maia, A. Quivy, and A. B. Henriques, Appl. Phys. Lett. **99**, 221914 (2011).
18. E. A. Zhukov, D. R. Yakovlev, M. Bayer, E. L. Ivchenko, G. Karczewski, T. Wojtowicz, and J. Kossut, Phys. Rev. B **76**, 205310 (2007).

Translated by E. Smorgonskaya